RELATION OF FRACTURE ENERGY OF SUB-SIZED CHARPY SPECIMENS TO STANDARD CHARPY ENERGY AND FRACTURE TOUGHNESS

Hans-Jakob Schindler and Peter Bertschinger
Mat-Tec SA, Unterer Graben 27, CH-8401 Winterthur, Switzerland

KEYWORDS: Charpy-V-notch test, sub-size specimens, fracture toughness, fracture energy, scaling laws, J-Integral, J-R-curve, impact testing, J-resistance curve, analytical relation

---

Abstract: The total fracture energy of edge-cracked beams under bending load is strongly dependent on specimen size, so the Charpy energy can only be measured on standard specimens. By means of a simplistic mechanical model a mathematical relation between the total fracture energy of an edge-cracked beam under bending and the fracture toughness is derived, from which a mathematical relation between the fracture energy and specimen size is obtained. It can be used to scale-up the fracture energy of sub-sized tests, and then use the evaluation procedure for standard Charpy specimens mentioned above. Unlike the commonly used empirical correlation formulas, the presented scaling law is applicable to any elastic-plastic material. It holds for the upper-shelf regime, and as a lower bound also in the brittle-to-ductile transition regime. The results are compared with experimental data obtained from different specimen sizes.

Nomenclature

a	crack length
A	Non-dimensional constant
a_0	initial crack length or notch depth, respectively
A_g	uniform fracture strain (strain at maximum force of a uniaxial tensile test)
B	specimen thickness
b_0	initial ligament width, $W-a_0$
C	constant
Δa	stable tearing crack extension
Δa_m	crack extension at maximum load
F_m	maximum load
J	J integral
$J_{0.2t}$	near-initiation J as defined in Fig. 3
J_{Ic}	critical J integral
K_{JKV}	Critical SIF calculated from $J_{0.2t}$ obtained from the KV-correlation
KV	Charpy fracture energy
KV’	Charpy fracture energy obtained by scaling-up a sub-sized test
p	exponent
R_m	ultimate tensile strength
R_p	yield stress (stress at 0.2% plastic strain)
σ_f	flow stress, $\sigma_f = (R_p+R_m)/2$
σ_{fd}	flow stress σ_f at increased strain rate (dynamic flow stress)
SIF	stress intensity factor
W	specimen width
W_m	energy consumed by the test specimen up to maximum load
W_{mp}	plastic (nonrecoverable) part of W_m
W_t	total fracture energy
E	Young’s modulus
Z	Standard reduction of area of a uniaxial tensile test (nondimensional)
ν	Poisson’s ratio

( )’ Quantity corresponding to another specimen size

1. Introduction

Because of its simplicity the standard Charpy test is still a very popular toughness test, although the measured quantity, the fracture energy KV, is known to be strongly dependent on specimen geometry, size, notch sharpness and loading rate. Therefore, the fracture energy of the standard specimen has neither a direct relation to the fracture energy of a structural part nor to fracture toughness in terms of K_{Ic} or J_{Ic}. The physical processes involved are rather different: In KV, there are contributions from processes like notch root blunting, ductile crack initiation, and, mainly, tearing crack growth, shear-lip formation and plastic deformation of the ligament, whereas J_{Ic} or K_{Ic} represent critical parameters of the corresponding local crack tip load and characterize just the resistance against crack extension. For these reasons KV rather serves as an “indicating” than a “quantifying” toughness parameter. Nevertheless, fracture toughness is often estimated from KV. A number of corresponding empirical correlations are offered in the literature [1-4]. However, for the reasons mentioned above, these correlations are considered to be rather unreliable and valid only with restriction to certain classes of materials.

Nevertheless, by means of some simplistic mechanical models, Schindler [5, 6, 7] derived a mathematical relation between the J-R-curve and the fracture energy in bending. Application of this general relation to the special case of the standard Charpy test lead to an analytical relation between KV and J_{Ic}, giving some theoretical justification to the empirical correlation formulas. Furthermore, the analytical relation shows additional influencing material parameters like flow stress and hardening exponent. It has been successfully applied to steels of different strength, aluminum and – as shown in the present paper – to several types of bronce.

In practical material testing there sometimes are situations where sub-sized specimens have to be used instead of standard ones. A typical miniature specimen is the KLST-specimen according to the German standard DIN 50 115, which has the size 4x3x22 mm, or the half-Charpy according to [ESIS1]. In order to interpret and classify the obtained fracture energy, there often is a need to compare them with standard data. However, the relation of the fracture energy of sub-sized specimens to the one of standard specimens is complex, including a significant, material-dependent temperature shift due to the reduced constraints, and a strongly non-linear size-dependence of the upper shelf energy. There are several empirical correlation formulas to relate the upper shelf fracture energy of sub-sized specimens to the one of standard Charpy energy [8, 9, 10]. The relation appears to be not only size- but also material-dependent.

In the present paper an analytical relation between the upper-shelf fracture energy of different specimen sizes is presented which can serve as a scaling law of Charpy-type fracture energy. It is experimentally confirmed by comparison of up-scaled fracture energy with directly measured ones for different materials.

2. Estimation of J-R Curve From Bend Test

As shown by the first author in [11, 12, 13] the J-R-curve can be estimated from the continuous force-displacement-diagram of a single, uninterrupted, static or dynamic bending test (Fig. 1 and 2) by

$$J(\Delta a) = C \cdot \Delta a^p \qquad \text{for } \Delta a < (W-a_0)/10 \qquad (1)$$

where

$$C = \left(\frac{2}{p}\right)^p \cdot \frac{h(a_0)}{B\,(W-a_0)^{1+p}} \cdot W_t^{\;p} \cdot W_{mp}^{\;1-p} \qquad (2)$$

$$p = \left(1 + \frac{W_{mp}}{2W_t}\right)^{-1} \tag{3}$$

W_{mp} and W_t are the dissipated energy at maximum force and the total fracture energy, respectively, that can be obtained from the load-displacement diagram (Fig. 2). The factor η is the well known η-parameter for the edge-cracked 3-point bending specimen, which is according to [8]

$$\eta = 13.81 \cdot \frac{a}{W} - 25.12 \cdot \left(\frac{a}{W}\right)^2 \qquad \text{für } 0<a/W<0.275 \tag{4a}$$

$$\eta = 1.859 + 0.03/(1-a/W) \qquad \text{für } a>0.275W \tag{4b}$$

The crack extension at maximum force F_m was obtained to be

$$\Delta a_m = \frac{W_{mp} \cdot p \cdot b_0}{2W_t} \tag{6}$$

According to eqs. (1-3) the J-R curve is determined by only two experimental parameters, W_{mp} and W_t, which can be easily determined from the force-displacement diagram even if it is disturbed by of by dynamic oscillations, as long as the behaviour is essentially quasistatic. Therefore this evaluation procedure is well-suited to be applied to testing at increased loading rates like typically Charpy-type testing.

3. Estimation of J-R Curve from a Non-Instrumented Test

In the case of a non-instrumented impact test like the classical Charpy test, the only available experimental value is the total fracture energy W_t. As shown in [6] and [7], by using the additional mathematical condition of maximum force, another equation for the crack extension at maximum force is obtained:

$$\Delta a_m = \frac{A_g \cdot p \cdot b_0}{2} \tag{6}$$

where A_g denotes the standard uniform fracture strain to be measured on a uniaxial tensile test as the plastic strain at maximum force. By comparison of (6) with (5), W_{mp} can be eliminated from (2) and (3), resulting in the following expressions

$$C = \left(\frac{2}{p}\right)^p \cdot \frac{\eta(a_0)}{B \cdot (W - a_0)^{1+p}} \cdot W_t \cdot A_g^{1-p} \tag{7a}$$

$$p = \left(1 + \frac{A_g}{2}\right)^{-1} \tag{7b}$$

Eq. (1), (7a) and (7b) enable the J-R curve to be determined just from the total fracture energy and the uniform fracture strain. By inserting the corresponding parameters of the standard Charpy tests, i.e. W_t = KV, B = W = 10 mm, a_0 = 2 mm and, according to eq. 4, η = 1.76, the J-R-curve is obtained from a single Charpy test in the upper shelf or upper transition range. The effect of the finite notch root radius is discussed in [6], and the corresponding correction is used in section 5 later on.

4. Scaling Law for Fracture Energy

Although the J(Δa)-curve determined by eqs. (1), (7a) and (7b) is just an extrapolation of the ductile tearing phase towards the blunting regime and not necessarily equivalent to the near-initiation J-R-curve of the material (see discussion in next section), it is expected to be size-independent in the range of J-controlled crack-tip-loading, i.e. Δa<W/10. Hence, from two specimens with different sets of geometrical parameters (W, B, a_0 for one specimen, W', B', a_0' for the other), the same value of the factor C as given in eq. (7a) should result. From this condition, one obtains from (7a) the following relation:

$$\frac{h(a_0/W)}{B\cdot(W-a_0)^{1+p}}\cdot W_t=\frac{h(a_0'/W')}{B'\cdot(W'-a_0')^{1+p}}\cdot W_t' \tag{8}$$

From the fracture energy W_t measured on a specimen with the geometrical parameters W, B, and a_0, the fracture energy W_t' of a specimen of a different size and shape (W', B', a_0') can be calculated as

$$W_t'=\frac{h(a_0/W)\cdot B'\cdot(W'-a_0')^{1+p}}{h(a_0'/W')\cdot B\cdot(W-a_0)^{1+p}}\cdot W_t \tag{9}$$

The parameter p is given in (7b). With some adequate simplification the above given scaling law applied to standard Charpy specimen results in

$$KV'=\frac{5.68}{B}\cdot h(a_0/W)\cdot\left[\frac{8}{(W-a_0)}\right]^{2-A_g/2}\cdot W_t \tag{10}$$

In this equation, KV' denotes the upper shelf or upper transition Charpy energy estimated from a Charpy-type test using a sub-sized (or over-sized, respectively) specimen with the dimensions B, W and a_0, which have to be inserted in millimeters. Some experimental validation of (10) is given in section 6.

In a similar way, using the corresponding relation given in section 2, scaling laws for further parameters of instrumented bending tests were obtained [13].

5. Determination of Fracture Toughness

KV' values determined from sub-sized specimens by means of (10) can serve to estimate fracture toughness in similar ways as from Charpy fracture energy KV. For this purpose, we suggest to use the semi-analytical relation between KV and J derived in [6, 7], rather than the common empirical correlation formulas. In the following this estimation procedure is roughly outlined.

In principle, the J-R curve estimated by (1), (7a) and (7b) can be used to determine approximate fracture toughness properties like the J_{Ic} or $J_{0.2Bl}$ from the J-R-curve, as defined in the corresponding standards like ASTM E 1820 or ISO/DIS 12135. However, one should keep in mind that the J(Δa)-curve according to the above derivation follows from an analytical treatment of the ductile tearing phase of crack extension, i.e. in the range $\Delta a>\Delta a_m$. The analysis is based on a mechanical model in which ductile tearing is assumed to be governed by a constant crack-tip opening displacement (see [6] for derivation). Therefrom the J(Δa)-curve in the range $\Delta a<\Delta a_m$ is obtained by extrapolation. For this reason it does not reflect the J(Δa)- behaviour in presence of the initially higher crack-tip constraints, which depend on the thickness and the initial crack length. For this reason it is expected that the real J-R-curve measured directly exhibits some deviation from the calculated one.

To account for the effect of the initial crack-length a_0, a constraint factor is introduced in [7] such that

$$J_R(\Delta a) = \frac{C}{k\left(\frac{a_0}{W}\right)} \Delta a^p \quad (11)$$

According to [7] a conservative empirical estimation of the constraint correction factor is

$$k(a_0/W) = 1 + 9 \cdot (0.5 - \frac{a_0}{W})^2 \qquad \text{for } a_0<0.5W \quad (12a)$$

$$\kappa(a_0/W) = 1 \qquad \text{for } a_0>0.5W \quad (12b)$$

Comparison with low-blow-data [10, 11, 14] revealed that the shape of the J-R-curve in the high-constraint initiation phase is improved by modifying the exponent p to

$$p = \frac{3}{4} \cdot \left(1 + \frac{W_{mp}}{W_t}\right)^{-1} \quad (13a)$$

for instrumented tests, or to

$$p = \frac{3}{4} \cdot \left(1 + A_g\right)^{-1} \quad (13b)$$

for non-instrumented tests, respectively.

When dealing with methods to estimate fracture toughness, it is advisable to use conservative definitions of the key parameters. For this reason, $J_{0.2t}$ as defined in Fig. 3 is suggested to be used instead of the standard $J_{0.2Bl}$ according to ISO 12135 (or J_Q according to ASTM E 1820, respectively). The former has a clearer physical meaning than $J_{0.2/Bl}$ or J_Q and can be represented in closed form in terms of C, as given below in (16). The blunting line, which is required to determine $J_{0.2t}$ as well as $J_{0.2/Bl}$ or J_Q, is defined according to the draft international standard ISO/DIS 12135 by

$$J = s_1 \cdot \Delta a \quad (14)$$

where

$$s_1 = 3.75 \cdot R_m \quad (15a)$$

with R_m denoting the ultimate tensile strength. Alternatively, the less conservative s_1 according to ASTM E1820 can be used, i.e.

$$s_1 = 2.0 \cdot \sigma_f \quad (15b)$$

where $s_f = (R_p+R_m)/2$ represents the flow stress. For impact tests we suggest to use rather (15a) than (15b), since the former tends to account for the increased flow stress due to high strain rates[1].

In mathematical terms, $J_{0.2t}$ as defined in Fig. 3 reads

[1] In the case of impact tests, the strength values like R_m or σ_f should be the ones at the corresponding strain rate. Nevertheless, since the derived formulas are just approximations, we suggest to use the quasistatic values.

$$J_{0.2t} = \frac{C}{\boldsymbol{k}(a_0/W)} \cdot \left[\left(\frac{C}{s_1} \right)^{1/_{1-p}} + 0.2mm \right]^p + \frac{K_I^2(F_m)}{E}(1-\boldsymbol{n}^2) \qquad (16)$$

The second term in (16) represents the elastic component of $J_{0.2t}$, which is, for the sake of simplicity, assumed to correspond to the elastic component of J at maximum load. In the case of classical (non-instrumented) Charpy tests, the latter is not known, so it is proposed in [6, 7] to estimate it from the plastic collapse condition. Based on ASTM E1820 this results in

$$F_m \cong F_0 \cong \frac{4 \cdot \boldsymbol{s}_f \cdot B \cdot (W - a_0)^2}{3S} \qquad (17)$$

Using the well-known SIF for a deeply cracked beam under bending [15], the SIF for an edge crack $a_0 > W/3$ under 3-point bending due to the force given in (17) is approximated by

$$K_I(F_m) \cong \frac{4 \cdot \boldsymbol{s}_f \cdot \sqrt{W - a_0}}{3} \qquad (18)$$

From J according to (16) a representative (conservative) fracture toughness value K_{JWt} can be derived by the well-known relation

$$K_{JWt} = (J_{0.2t} \cdot E/(1-n^2))^{1/2} \qquad (19)$$

If the fracture energy W_t corresponds to KV determined by a standard Charpy test, the estimated fracture toughness K_{JWt} is suggested to be denoted as K_{JKV}. Introducing the values of the parameters corresponding to the standard Charpy specimen, the following equation to determine fracture toughness K_{JKV} from KV or KV' is obtained:

$$K_{JKV} = \sqrt{ \frac{C \cdot E}{(1-\boldsymbol{u}^2)} \cdot \left[\left(\frac{C}{3.75 \cdot R_m} \right)^{1/_{1-p}} + 0.2mm \right]^p + 7.15 \cdot \boldsymbol{s}_f^2 } \qquad (20)$$

where

$$C = \frac{0.0250}{8^p} \cdot (KV - \frac{7.97 \cdot \boldsymbol{s}_f \cdot Z}{1-Z}) \cdot A_g^{1-p} \qquad (21)$$

$$p = \frac{3}{4} \cdot (1 + A_g)^{-1} \qquad (22)$$

The second term in the bracket of (29) accounts for the effect of the finite notch root radius of the Charpy specimen, as shown in [6]. Therein, Z denotes the reduction in area of a uniaxial tensile test. Like A_g, Z has to be inserted as a non-dimensional number (not as a percentage), and KV in N·mm.

6. Experimental Validation

6.1. Scaling of fracture energy

To verify the formulas derived above the fracture energy measured on sub-sized specimens is scaled-up to standard sized specimens by means of (9) and compared with directly measured standard Charpy fracture energy for materials of different toughness. From the latter, fracture toughness is estimated by means of (19) and compared with directly measured fracture toughness. The materials and specimen sizes used for these comparisons are shown in Table 1 and 2. The two considered types of bronce had the same chemical decomposition, but differing mechanical properties due to different heat treatment.

The measured fracture energy W_t (mean values from 3 – 5 specimen each) are given in Table 3.

TABLE 1: *Geometry of the used specimens (see Fig. 1).*

	B [mm]	W [mm]	b_0 [mm]	S [mm]	ç
standard Charpy	10	10	8	40	1.76
KLST	3	4	3	22	1.88
Half-size Charpy	5	5	4	22	1.76

TABLE 2: *Material properties of the tested materials*

	R_m [N/mm^2]	R_p [N/mm^2]	A_g [-]	Z [-]	E [N/mm^2]
Steel A533 B	640	470	0.11	0.55	210000
Bronce GZ-CuSn12Ni (Type 1)	299	178	0.11	0.12	120000
Bronce GZ-CuSn12Ni (Type 2)	477	208	0.5	0.43	130000

Table 4 shows the W_t values given in Table 1 scaled up to the size of standard Charpy specimens obtained by using formula (10). Compared with the directly measured Charpy fracture energy given in Table 3, the deviations given in percentages in Table 4 are obtained. Regarding the facts that these formulas are purely theoretically derived, without any adjustable factor, and that the (natural) scatter of the Charpy energy is usually as much as up to ±5%, the agreement between measured and scaled fracture energy is very satisfying.

TABLE 3: Experimental W_t-values measured on standard and sub-sized specimens

	standard Charpy	KLST	Half-size
Steel A355	215 J	8.42 J	29.4 J
Bronce Type 1	5.9 J	0.264 J	-

TABLE 4: Fracture energy KV' estimated from W_t of sub-sized specimens by eq. (10)

	KLST		Half-size	
	W_t'	deviation	W_t'	deviation
Steel	203 J	-3.62%	227 J	+5.5%
Bronce Type 1	6.35 J	+7.6%	-	-

6. 2. Estimation of Fracture Toughness

Applied to steel, the reliability of eqs. (20) – (22) to estimate fracture toughness was shown elsewhere [6, 7]. Being derived semi-analytically, the applicability of (20) – (22) is not restricted to steel, but in principle open to any elastic-plastic material. In the following we show some comparison of measured and predicted fracture toughness for two heat-treatments of bronze GZ-CuSn12Ni, denoted by type 1 (coarse grained) and type 2 (fine grained), where the former is similar to the type considered in the previous section (Table 2). In Table 5 the fracture toughness measured according to ASTM E1820 is compared with the one estimated from the Charpy fracture energy KV by means of (20) – (22). The agreement is surprisingly good, indicating that the relation between KV and fracture toughness, which forms the basis of the scaling law derived above, is indeed applicable to any type of elastic-plastic materials.

TABLE 5: Comparison of fracture toughness predicted by means of eq. (20) – (22) with standard values K_{Jc} for the considered two types of bronze.

Material	KV [J]	K_{Jc} measured [N/mm$^{1.5}$]	K_{JCV} predicted [N/mm$^{1.5}$]
Bronze Serie 292	6.1	1084	1031
Bronze Serie 200	32	3842	3671

7. Discussion and Conclusions

By the presented formula it is possible to estimate the J-R-curve or fracture toughness from the fracture energy of an edge-cracked or sharply notched beam of any size under static or impact bending. A typical application is the estimation of fracture toughness from standard or sub-sized Charpy specimens However, to estimate fracture toughness from a sub-sized Charpy-type test, it is advisable to proceed in two steps: First, the measured fracture energy should be transferred to the standard size. For this purpose, a scaling law for the total fracture energy has been derived analytically based on simple mechanical models. Second, the obtained Charpy energy shall be used to estimate the fracture toughness. This can be done using the semi-analytical relation derived in [6, 7]. Estimation of $J_{0.2t}$ directly from the sub-sized test is not recommended, because the empirical modification of p as given by (13a) or (13b) corresponds to the standard specimen. It is expected to be somewhat different for other specimen sizes.

The underlying mechanical model is based on the assumption that the involved fracture processes are predominately ductile tearing. Thus, the J-R-curve represented by (1) or (7a) as well as the scaling law (10) are restricted to the upper shelf regime from a theoretical point of view. Nevertheless, they ca be formally applied in the ductile-to-brittle transition (DBT) range and on the lower shelf as well. Although lacking a physical basis the near initiation toughness defined in (16) or (20) represent mathematically lower-bound values in these toughness ranges, as shown in [6], so conservative approximations of fracture toughness are expected to result. However, one has to be aware, that in general there is a significant shift of DBT-temperature due to specimen size, which has to be accounted for. Some empirical data on this subject are given in [8, 9]. Furthermore, the J-R-curve and fracture toughness is in general rate dependent, so the loading rate in terms of dJ/dt or dK_I/dt should be also provided in the test report.

Of course, analytical relations are approximations in any case, because they are based on simplifying analytical models. Nevertheless, in combination with experimental data, they can be used to establish semi-empirical relations that are much more general and reliable than purely empirical relations.

Literature

[1] Server, W.L., “Static and Dynamic fibrous initiation toughness results for nine pressure vessel materials,” Elastic-Plastic Fracture, ASTM STP 668, J.D. Landes, et al., Eds., American Society for Testing and Materials, West Conshohocken, PA, 1979, pp. 493-514

[2] Norris, D.M., Reaugh, J.E. and Server, W.L., “A fracture toughness correlation based on Charpy initiation energy,” Fracture Mechanics: 13th Conference, ASTM STP 743, R. Roberts, Ed., American Society for Testing and Materials, West Conshohocken, PA, 1981, pp. 207-217.

[3] Barsom, J.M. and Rolfe, S.T., Fracture and fatigue Controle in Structures – Application of Fracture Mechanics, 2nd ed., Prentice-Hall. Englewood Cliffs, NJ, 1987

[4] Sailors, R.H. and Corten, H.T., “Relationship Between Material Fracture Toughness Using Fracture Mechanics and Transition Temperature Tests, Proc. of the 1971 National Symposium on Fracture, ASTM STP 514, American Society for Testing and Materials, West Conshohocken, PA,1972, p. 164-191

[5] Schindler, H.J., The correlation between Charpy fracture energy and fracture toughness from a theoretical point of view, Proc. 12th European Conference on Fracture, Sheffield, 1998, 841-847

[6] Schindler, H.J., “Relation Between Fracture Toughness and Charpy Fracture Energy - An Analytical Approach”, Pendulum Impact Testing: A Century of Progress, ASTM STP 1380, T. Siewert and M. P. Manahan, Sr., Eds., American Society for Testing and Materials, West Conshohocken, PA, 1999, 337-353

[7] Schindler, H.J., Abschätzung von Bruchzähigkeitskennwerten aus der Bruch- oder Kerbschlagarbeit, Materialwissenschaft und Werkstofftechnik, Vol. 32, No. 6, 2001

[8] Lucon, E., et al., Characterizing Material Properties by the Use of Full-Size and Sub-Size Charpy Tests”, Pendulum Impact Testing: A Century of Progress, ASTM STP 1380, T. Siewert and M. P. Manahan, Sr., Eds., American Society for Testing and Materials, West Conshohocken, PA, 1999, pp. 146 - 163

[9] Lucon, E., “European Activity on Instrumented Impact Testing of Sub-Size Charpy V-Notch Specimens”, Pendulum Impact Testing: A Century of Progress, ASTM STP 1380, T. Siewert and M. P. Manahan, Sr., Eds., American Society for Testing and Materials, West Conshohocken, PA, 1999, pp. 242-252

[10] Corowin, W.R., and Houghland, A.M., “Effect of specimen size and material condition on the Charpy impact properties of 9Cr-1Mo-V-Nb steel”, The Use of Small-Scale Specimens for Testing Irradiated Material, ASTM STP 888, Philadelphia, 1986, pp. 325-338

[11] Schindler, H.J., “Estimation of the dynamic J-R curve from a single impact bending test,” Proc. 11th European Conf. on Fracture, Poitiers, 1996, EMAS, London, pp. 2007-2012

[12] Schindler, H.J., et al, “Ageing an Irradiation Surveillance by Means of Impact Testing of Pre-Cracked Charpy Specimens”, Proc. Int. Symposium on Materials Ageing and Life Management, Ed. B. Raj, et al., Kalpakkam, India, Oct. 2000, 837-846

[13] Schindler, H.J, Veidt, M., Fracture Toughness Evaluation from Instrumented Sub-size Charpy-Type Tests, in: Small Specimen Test Techniques, ASTM STP 1329, W.R. Corowin, et al., Eds., 1998, 48 – 62

[14] Böhme, W. and Schindler, H.J. "Application of Single Specimen Methods on Instrumented Charpy Tests: Results of DVM Round Robin Exercises," *Pendulum Impact Testing: A Century of Progress*, *ASTM STP 1380*, T. Siewert and M.P. Manahan, Eds., American Society for Testing and Materials, West Conshocken, 1999

[15] Tada, H., Paris, P.C. and Irwin, G.R. (1973) *The Stress Analysis of Cracks Handbook*. Del Research Corp., St. Louis.

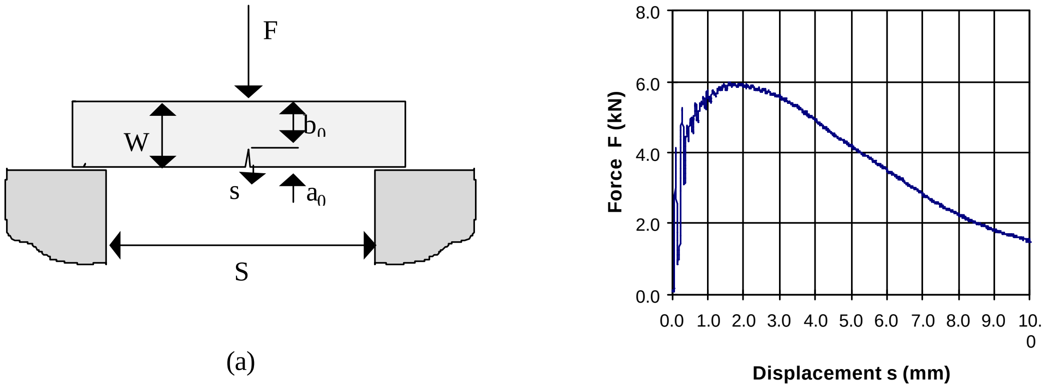

Fig. 1 - *Mechanical system (a) and the corresponding force-displacement diagram of a bending test with an edge-cracked specimen in the upper-shelf range (b).*

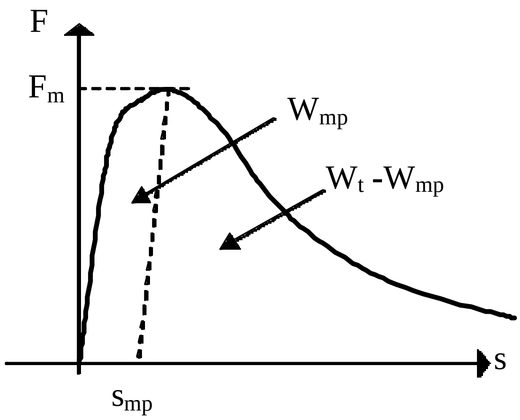

Fig. 2 –*Quasistatic Force-deflection diagram of an instrumented Charpy test (schematic)*

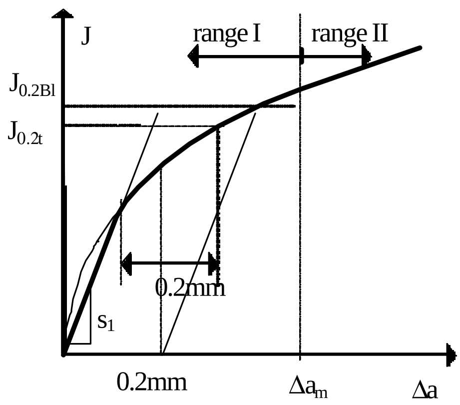

Fig. 3 - *J-R curve and definition of near-initiation values $J_{0.2Bl}$ and $J_{0.2t}$*